Front. Phys. China (2006) 4: 442－445
DOI 10.1007/s11467-006-0046-4

RESEARCH ARTICLE

**PANG Qi, ZHAO Li-juan, GE Wei-kun, WANG Jian-nong,
FANG Yue-ping, WEN Xiao-gang, YANG Shi-he**

Vertically aligned and hexagonal crystal ZnSe nanoribbon arrays on Zn substrates

Abstract The vertically aligned and hexagonal ZnSe nanoribbon array can be easily obtained by heating ZnSe: 0.38 en precursors (en = ethylenediamine), while ZnSe precursor nanoribbon arrays are grown directly on Zn foils in en using the solvothermal method. The nanoribbons are mostly about 4 nm in thickness, 100－300 nm in width, and 2 μm in length. The characteristics observed using scanning electron microscopy and X-ray diffraction indicate that the ZnSe precursor as well as ZnSe nanoribbons are vertically aligned on almost the whole zinc foil surface and form a large-scale uniform array. Particularly, ZnSe precursor nanoribbons are hybrid materials of ZnSe and en, while ZnSe nanoribbons are in the from of hexagonal structures. Possible growth mechanisms of the ZnSe precursor nanoribbon arrays are also proposed.

Keywords nanoribbon, vertically aligned, hexagonal, growth mechanism

PACS numbers 81.07.Bc, 81.10.Dn, 81.20.Ka, 82.20.-w

1 Introduction

ZnSe is of great importance for short-wavelength lasers and other optoelectronic applications. As a Zn-based II-VI compound, ZnSe is a direct band gap semiconductor with room-temperature band gap energy of 2.8 eV. Therefore, ZnSe has attracted great interest in the field of thin films, quantum wells, and bulk crystals material researches [1－6]. ZnSe-based optoelectronic devices have also been the subject of intensive study [7]. In the field of nanoelectronics, one-dimensional (1D) semiconductor nanomaterials are considered to be key structural components of electronic, magnetic, and photonic devices. The formation of well-aligned arrays of 1D nanomaterial is particularly important because it will eventually affect their optical and transport properties [8－14]. In comparison that nanowires, the nanoribbons that have a distinct rectangular cross-section and a large width-to-thickness ratio offer exciting opportunities for both technological applications and fundamental studies. Recently, Huang *et al*. [15, 16] prepared a so-called inorganic–organic ZnSe $en)_{0.5}$, ZnTe $(en)_{0.5}$ slabs via a solvothermal process using $ZnCl_2$ as zinc source and ethylenediamine (en) as solvent; Deng *et al*. [17] also prepared the ZnS and ZnSe precursors lamellar via a solvothermal process using zinc powder or $ZnCl_2$ as zinc source and en as solvent; Jiang *et al*. [18] reported the synthesis of ZnSe nanoribbon and nanowires using laser ablation of ZnSe pressed powders. However, these recent syntheses of ZnSe or ZnSe precursor nanoribbons (lamellas or slabs) are randomly orientated rather than aligned arrays. So far, to our knowledge, no ZnSe nanoribbon arrays have been synthesized. Here, we report the use of Zn foil as Zn source via a solvothermal method to fabricate well-aligned ZnSe precursor nanoribbon arrays on zinc surface. Through further heat treatment we have achieved the transformation of the ZnSe precursor nanoribbon arrays to ZnSe nanoribbon arrays without obvious morphological changes. In addition, the resulting ZnSe nanoribbons are in the form of hexagonal structures.

PANG Qi, ZHAO Li-juan, GE Wei-kun, WANG Jian-nong (✉)
Physics Department, The Hong Kong University of Science and Technology,
Clear Water Bay, Hong Kong, China
E-mail: phjwang@ust.hk

FANG Yue-ping, WEN Xiao-gang, YANG Shi-he
Chemistry Department, The Hong Kong University of Science and Technology, Clear Water Bay, Hong Kong, China

Received September 18, 2006

2 Experiment

A typical solvothermal synthesis of ZnSe precursor nanorib-

bon was carried out as follows. At the beginning, zinc foils (10 mm × 10 mm × 0.25 mm) with a purity of 99.9 % (Aldrich) were washed in ethanol. The washed zinc foils were mixed with 0.1 g Se powder in a 25 mL Teflon-lined stainless steel autoclave; then the autoclave was filled with 17 ml en. Afterward, the autoclave was heated up and maintained at 140 °C for 24 h. A light yellow-colored layer was formed on the surface of the zinc foil. It was washed with de-ionized water and ethanol three times, respectively, and dried in N_2 for further characterizations. The ZnSe nanoribbon arrays on Zn foil were then obtained by heating the as-prepared ZnSe precursor nanoribbon in N_2 at 300 °C for ~5 h.

The as-prepared products (ZnSe precursor nanoribbon arrays) and the annealed products (ZnSe nanoribbon arrays) were characterized directly on the Zn foil by scanning electron microscopy (SEM) and X-ray diffraction (XRD). For transmission electron microscopy (TEM) observations, the products were first treated by ultra sonic ally bathing the Zn foil with the products on it in ethanol for 20 min and products on the Zn foil were first treated by ultra-sonic bathing in ethanol for 20 min, and then by dispersing it onto the carbon lacy film on a Cu grid. For infrared absorption (IR) experiment, the samples were obtained by scraping off the products from the Zn foil. The XRD analyses were performed on a Philips PW-1830 X-ray diffractometer with Cu Kα irradiation (λ = 1.5406 Å) at a scanning speed of 0.025 deg/s over the 2θ range of $10^{\circ}-70^{\circ}$. The morphologies of the samples were characterized using a JEOL 6300 SEM and JEOL 6700F SEM at an accelerating voltage of 15 kV. TEM observations were carried out on a JEOL 2010F microscope operated at an accelerating voltage of 200 kV. Infrared absorption spectra were obtained on a Perkin-Elmer Spectrum GX FTIR spectrometer. Thermo-gravimetric analysis (TGA) was carried out under N_2 at a heating rate of 10 °C /min using NETZSH TG-209 instrument.

3 Results and discussions

Figure 1 (a) shows a typical top view SEM image of the asprepared products, ZnSe precursor nanoribbon arrays, on a zinc foil. As can be seen, the entire zinc foil surface is uniformly covered by the nanoribbons. The higher-magnification image [Fig. 1 (a) inset] shows that the nanoribbons are rather smooth with a typical width of 100 ~ 400 nm. A side view of the sample [Fig. 1 (b)] demonstrates that, in particular, the nanoribbons are vertically aligned on the zinc foil surface and form a large-scale uniform array. A typical TEM micrograph of the ZnSe nanoribbon precursor [Fig. 1 (c)] illustrates that these nanoribbons are about 300 nm in width and a few nm in thickness and most of the nanoribbons have a uniform width.

The composition and structure of the ZnSe precursor nanoribbons are studied by infrared (IR) absorption spectroscopy, thermo-gravimetric (TGA) analysis, and X-ray diffraction (XRD). Figure 2 shows the IR absorption spectra from the ZnSe precursor, pure en, and the annealed ZnSe products, respectively. In comparison with that of the pure en, the spectrum of the ZnSe precursor exhibits characteristic N-H vibration bands of pure en as marked by arrows. since ZnSe has no vibration bands within the measurement range, these results indicate that the ZnSe precursor is a mixture of ZnSe and en. The red shifts of the N-H stretching vibrations bands above 3000 cm^{-1} in the ZnSe precursors may result from the chemical bonding action between Zn^{2+} and N atom. Figure 3 shows the TGA results conducted in N_2 flow. A weight loss of 13.6 % up to 400 °C is observed. This weight loss is related to the removal of en molecules. Assuming the chemical formula for the precursor being ZnSe: x en, calculations based on the weight losses lead to $x \approx 0.38$. Furthermore, the XRD spectrum of the ZnSe precursor is shown in Fig. 4 (a). The strong and sharp diffraction peaks related to the ZnSe precursor reveal that it is well crystallized. However, these peaks cannot be indexed to any known phase of Se or ZnSe provided in the standard JCPDS cards except the Zn peaks from the substrate. All of the aforementioned results suggest that the ZnSe precursor nanoribbons obtained in our experiment are ZnSe and en hybrid material.

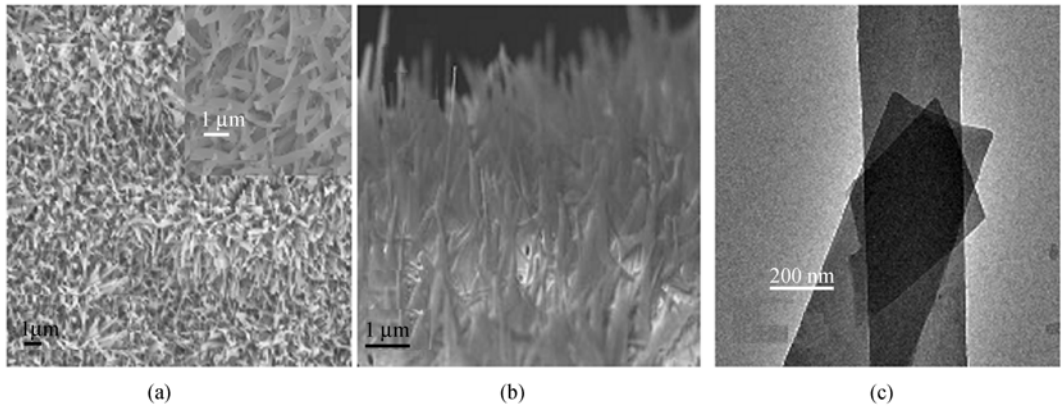

Fig. 1 SEM and TEM images of a ZnSe precursor nanoribbons array grown on a Zn foil. **(a)** A top view SEM low magnification image (Inset is a high magnification image); **(b)** A side view SEM image; **(c)** TEM image of ZnSe precursor nanoribbons.

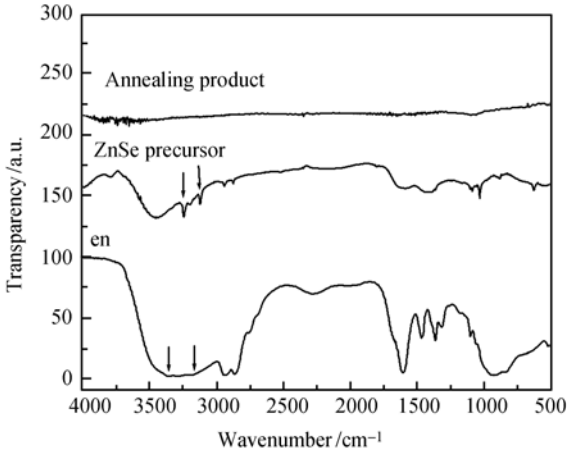

Fig. 2 IR absorbance spectra of en, the ZnSe precursor nanoribbon sample, and ZnSe nanoribbon sample, respectively, as indicated.

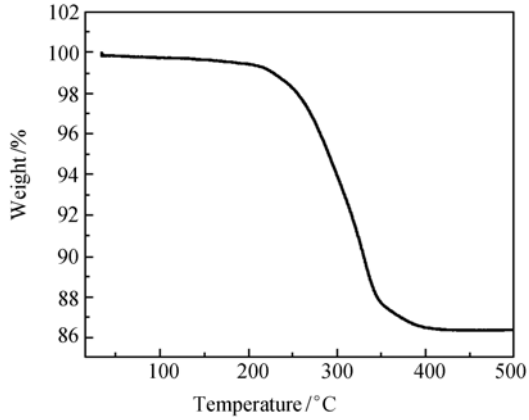

Fig. 3 TGA curve of ZnSe precursor nanoribbon sample.

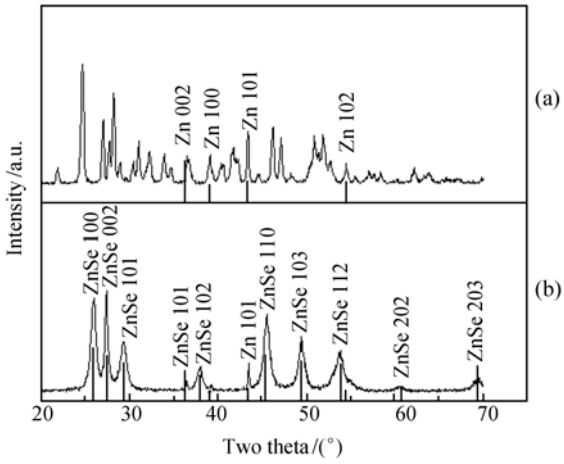

Fig. 4 X-ray diffraction spectra for **(a)** the ZnSe precursor nanoribbons and **(b)** ZnSe nanoribbons obtained by annealing the precursor nanoribbons in N_2 at 300 °C for ~5 h. The peaks are indexed to be the wurtzite (W) phase ZnSe.

The ZnSe: 0.38 en nanoribbon arrays can be fully converted into ZnSe nanoribbon arrays by thermal annealing. As can be seen in the IR spectrum of the annealed ZnSe nanoribbons (see Fig. 2) no en associated vibration bands are observed in comparison with the spectrum of pure en. The XRD spectrum of the annealed sample [see Fig. 4 (b)] also reveals that the ZnSe: 0.38 en precursor has been fully converted to ZnSe. The diffraction peaks can be indexed to the bulk ZnSe with wurtzite structures as indicated in Fig. 4 (b). The morphology of the annealed ZnSe nanoribbon arrays are displayed in Fig. 5. As can be seen in Fig. 5 (a), the ribbon like morphology is well preserved after annealing. Especially, the ZnSe nanoribbons are well aligned on the Zn foil substrate. The TEM image [Fig. 5 (b)] indicates that the crystallinity of the nanoribbon is improved.

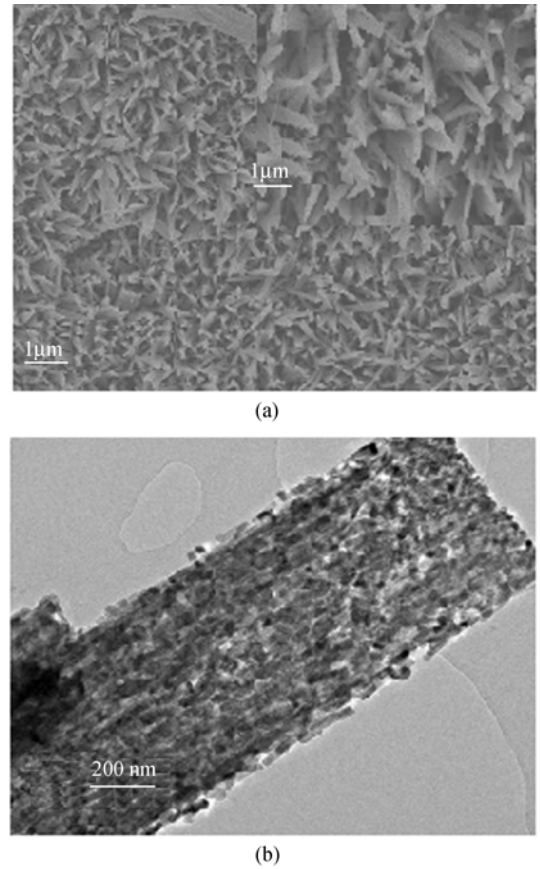

Fig. 5 SEM and TEM images of a ZnSe nanoribbons array on a Zn foil obtained by annealing the precursor nanoribbons in N_2 at 300 °C for ~5 h. **(a)** SEM low magnification image (top view) and high magnification image (inset); **(b)** A typical TEM image of ZnSe nanoribbon.

We believe that en used in our experiment acts both as the connecting molecular bridges between neighboring ZnSe layers and the surface-passivating agent in the formation of the ZnSe precursor nanoribbons. It has been reported [19] that en is a structure directing coordination molecular template (SCMT) responsible for the morphologies of II-VI semiconductors formed via solvothermal route using en as a liquid media. In our case, we think that en has played a similar role as SCMT. However, the nanoribbons synthesized in our process are almost vertically aligned arrays on

the Zn foil rather than the randomly orientated as synthesized by others [20, 22]. This leads us to propose that the growth procedure ZnSe precursor nanoribbon array in our case is related to both electrochemical reaction and SCMT mechanism. The overall reaction that accounts for the formation of ZnSe:en is probably as follows:

$$Zn + Se + (en)_n \rightarrow ZnSe{:}(en)_n \quad (1)$$

This overall reaction is analogous to the reaction-forming complexes of $ZnS_6(N\text{-}MeIm)_2$ reported by Rauchfuss [23]. We believe that in our process the overall reaction (1) is fulfilled via two electrochemical half-reactions as following:

$$2\,Zn - 4\,e + 4\,en \rightarrow 2\,Zn(en)_2^{2+} \quad (2)$$

$$Zn(en)_2^{2+} + 2Se + 4\,e \rightarrow 2\,ZnSe{:}(en)_x \quad (3)$$

As shown in Fig.6, these two half-reactions take place on the surface of the Zn foil at separate locations in space. First, the oxidation reaction at the Zn surface provides the Zn^{2+} ions and the complex of Zn $(en)_2^{2+}$ may be formed as the Zn^{2+} ions coordinate with en. Then, Se may react with this complex to form ZnSe:en nanoparticles. Finally, a large amount of ZnSe precursor particles nucleate on the Zinc foil surface to form ribbons. In this process, the Zn foil is the anode while the ZnSe precursor ribbons are the cathodes. The vertical growth of the ribbons continues as the complex of Zn $(en)_2^{2+}$ constantly diffuses to the cathode regions and reacts with Se to form ZnSe:en nanoparticles deposited on the ribbons.

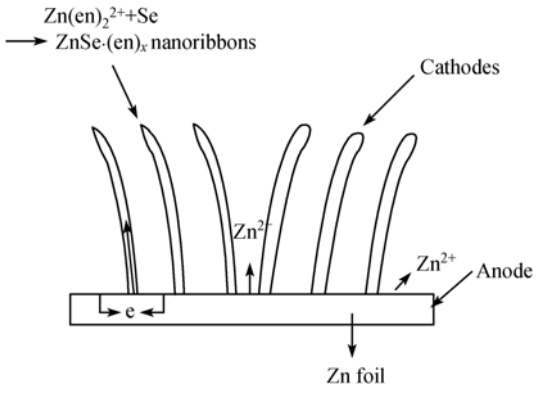

Fig. 6 Schematic illustration of the formation process of ZnSe precursor nanoribbon arrays.

Acknowledgements The authors appreciate the financial support extended by the Research Grant Council of Hong Kong SAR via grant number HKUST6069/02P. They also thank the MCPF of HKUST for the assistance in the sample characterizations.

References

1. Gutowski J., Michler P., Ruckmann H. I., Breunig H. G., Rowe M., Sebald K., and Voss T., Phys. Status Solidi B, 2002, 234 (1): 70
2. Garcia J. A., Remon A., Zubiaga A., Munoz-Sanjose V., and Martinez-Tomas C., Phys. Status Solidi A , 2002, 194 (1): 338
3. Burov L. I., Ryabtsev G. I., Smal A. S., and Waraxe I. N., Appl. Phys. B, 2002, 75: 63
4. Su C. -H., George M. A., Palosz W., Feth S., and Lehoczky S. L. J., Cryst. Growth, 2000, 213: 267
5. Kato H., Udono H., and Kikuma I. J., Cryst. Growth, 2001, 229: 79
6. Tournie E., Morhain C., Neu G., Faurie J. P., Triboulet R., and Ndap J. O., Appl. Phys. Lett., 1996, 68: 1356
7. Lischka K., Phys. Status Solidi B, 1997, 202: 673
8. Holmes J. D., Johnston K. P., Doty R. C., and Korgel B. S., Science, 2000, 287:1471
9. Wang S. H. and Yang S. H., Chem. Mater., 2001, 13: 4794
10. Wen X. G., Zhang W. X., Yang S. H., Dai Z. R., and Wang Z. L., Nano Lett., 2002, 2: 1397
11. Zhang W. X., Wen X. G., Yang S. H., Berta Y., and Wang Z. L., Adv. Mater., 2003, 15: 822
12. Wen X. G., Xie Y. T., Choi C. L., Wan K. C., Li X. Y., and Yang S., Langmuir, 2005, 21: 4729
13. Wen X. G., Wang S. H., Ding Y., Wang Z. L., and Yang S. H., J. Phys. Chem. B, 2005, 109: 215
14. Gudiksen M. S., Lauhon L. J., Wang J., Smith D. C., and Lieber C. M., Nature (London), 2002, 415: 617
15. Huang X. Y., Li J., and Fu H. X., J. Am. Chem. Soc., 2000, 122: 8789
16. Huang X. Y., Harry R. Heulings IV, Vina Le, and Li J., Chem. Mater., 2001, 13: 3754
17. Deng Z. -X., Wang C., Sun X. -M., and Li Y. -D., Inorganic Chemistry, 2002, 41 (4): 869
18. Jiang Y., Meng X. -M., Yiu W. -C., Liu J., Ding J. -X., Lee C. -S., and Lee S. -T., J. Phys. Chem. B, 2004, 108: 2784
19. Li Y. D., Liao H. W., Ding Y., Fan Y., Zhang Y., and Qian Y. T., Inorg. Chem., 1999, 38: 1382
20. Deng Z. -X., Wang C., Sun X. -M., and Li Y. -D., Inorganic Chemistry, 2002, 41 (4): 869
21. Jiang Y., Meng X. -M., Yiu W. -C., Liu J., Ding J. -X., Lee C. -S., and Lee S. -T., J. Phys. Chem. B, 2004, 108: 2784
22. Dev S., Ramli E., Rauchfuss T. B., and Wilson S. R., J. AM. Chem. Soc., 1990, 112: 6385